

are all substantially larger than the calorimetrically determined value for the first Mo=O bond dissociation energy in Mo(O)₂-(Et₃dte)₂ of 96 ± 3 kcal/mol.³⁷ The molybdenum value seems low, in comparison with the average D(Mo=O) in MoO₃ (g) of 141 kcal/mol³⁶ and given that Mo(O)(Et₂dte)₂ will quantitatively deoxygenate Ph₃AsO for which D(As=O) = 103 ± 7.^{38,39}

It is interesting to note that Me₂SO will oxidize both Re(III) (7) and Re(V) ([2]Cl) and that PPh₃ will reduce both Re(VII) ([3]BPh₄) and Re(V) ([1]BPh₄). This contrasts with molybdenum oxo systems such as Mo(O)₂dte₂ in which PPh₃ will reduce Mo(VI) but not Mo(IV).² Similarly, WCl₂(PMePh₂)₄ appears to be a much more avid oxygen atom acceptor than W(O)Cl₂(PMePh₂)₃.⁴⁰ Reaction 3 cannot, however, be used to estimate a bond strength in the rhenium(VII) species because [2]Cl → [3]Cl requires both an oxygen atom and an oxide ion. Similarly, [3]Cl → [2]Cl requires both an oxygen atom acceptor and a Lewis or protic acid to accept an oxide ion. (Of course, the rhenium itself can act as the acid with the formation of dimers or clusters.) In essence, the redox stoichiometry (two electron change) does not match the

oxo stoichiometry (mono-oxo → tri-oxo). This may be the reason why [3]Cl is reduced by ⁿBuNC only in the presence of Me₃SiCl as a Lewis acid.²³ The noncomplementarity of oxygen and electron stoichiometry is a common occurrence in oxo chemistry and is a reason for the often complex mechanisms observed.⁴¹

The oxidation of [1]Cl to Re(VII) by aqueous nitric acid requires more than 40 days at 80 °C, while [2]Cl is oxidized within an hour at 25 °C. This dramatic difference in the ease of oxidation is difficult to understand because the metal complexes differ only in that 1 has the Me₃tacn ligand and 2 has tacn. The driving force for oxidation should be similar for the two compounds, indicating a kinetic effect. The oxidation of [1]Cl is accelerated by the presence of Ag⁺, suggesting chloride dissociation, although the faster rate for the complex of the smaller ligand (tacn vs Me₃tacn) is not typical of dissociative processes. A conjugate base mechanism involving deprotonation of an N-H proton (common in cobalt(III) chemistry⁴²) is ruled out by the observation that the oxidation of [2]Cl is faster in acid than in base. The tacn N-H groups might enhance the rate by directing the solvent water to assist in Cl⁻ dissociation, as suggested in other cobalt ammine chemistry.⁴² It is also possible that oxygen atom transfer to [2]Cl is associative in character, which is prevented by the larger Me₃tacn ligand in [1]Cl. Further studies are in progress to probe the influence of ancillary ligands on the kinetics and thermodynamics of oxygen atom transfer.

Acknowledgment. We thank Dr. Rasmy Talaat for obtaining the FAB mass spectra and Professor Wiegardt for a preprint of ref 22a. This work was supported by the National Science Foundation, the Chevron Research Co., BP America, the Exxon Education Foundation, and the donors of the Petroleum Research Fund, administered by the American Chemical Society.

- (36) Glidewell, C. *Inorg. Chim. Acta* **1977**, *24*, 149-157. E.g. for WO₃ (in kcal/mol): D(O₂W-O) = 143; D(OW-O) = 147; D(W-O) = 161. The average binding energy of an oxygen atom in Re₂O₇ is 150 kcal/mol, calculated by dividing ΔH° for Re₂O₇(g) → 2Re(g) + 7O(g) by seven, but this is not a meaningful value because there are six multiple bonds and two single bonds in Re₂O₇.
- (37) Watt, F. D.; McDonald, J. W.; Newton, W. E. *J. Less-Common Met.* **1977**, *54*, 415-423.
- (38) (a) Barnes, D. S.; Burkinshaw, P. M.; Mortimer, C. T. *Thermochim. Acta* **1988**, *131*, 107-113. (b) D(As-O) has also been determined to be 106 ± 6 by Tsvetkov, V. G.; Aleksandrov, Y. A.; Glushakova, V. N.; Skorodumova, N. A.; Kol'yakova, G. M. *J. Gen. Chem. USSR (Engl. Transl.)* **1980**, *50*, 198-201.
- (39) The discrepancy between D(Mo=O) and D(As=O) has been noted by Holm,² who suggested that the arsenic-oxygen bond strength might be in error. However, the second determination of D(Ph₃As=O)^{38a} and the gas phase value for MoO₃ suggest that the actual molybdenum value may lie toward the high end of the reported error range.
- (40) Su, F.-M.; Bryan, J. C.; Jang, S.; Mayer, J. M. *Polyhedron* **1989**, *8*, 1261-1277. See also ref 35.

- (41) Beattie, J. K.; Haight, G. P., Jr. *Prog. Inorg. Chem.* **1972**, *17*, 93-145.
- (42) Basolo, F.; Pearson, R. G. *Mechanisms of Inorganic Reactions*, 2nd ed.; Wiley: New York, 1967; pp 134-135 (solvent assisted dissociation); and pp 415-416 (conjugate base mechanism).

Contribution from the Department of Chemistry, University of Florence, Via G. Capponi 7, I-50121 Florence, Italy, and Institute of Agricultural Chemistry, University of Bologna, Viale Berti Pichat 10, I-40127 Bologna, Italy

¹H NOE and Ligand Field Studies of Copper-Cobalt Superoxide Dismutase with Anions

Lucia Banci,[†] Alessandro Bencini,[†] Ivano Bertini,^{*†} Claudio Luchinat,[‡] and Mario Piccioli[†]

Received August 17, 1990

The ¹H NOE's on bovine erythrocyte Cu(II)₂Co(II)₂ superoxide dismutase in the presence of saturating amounts of azide have been measured and compared with those in the absence of azide. The interproton distances involving the histidines coordinated to copper(II) are quite similar. Efforts are made to minimize the errors in distances in order to obtain a reliable picture of the reciprocal positions of the above histidines. The conclusion that the histidine positions do not change upon anion binding is extended to the cases of CN⁻, NCO⁻, NCS⁻, and F⁻. Within this frame the essential disappearance of the hyperfine coupling between the protons of histidine-48 and the unpaired electron on copper(II) upon azide binding and the large variations of circular dichroism spectra are accounted for on the basis of an angular overlap treatment. The same model is used to discuss the spectral variations occurring in the cyanide and cyanate derivatives. It is proposed that the copper-nitrogen (His-48) distance increases upon anion binding as a result of a movement of the copper ion. The fluoride and thiocyanate derivatives are included in the present general model.

Introduction

Steady-state ¹H nuclear Overhauser effects (NOE) in paramagnetic metalloproteins can nowadays be measured,¹⁻³ and they potentially provide structural information in solution. We have measured ¹H NOE's on copper-cobalt superoxide dismutase (Cu₂Co₂SOD) and successfully related the X-ray interproton distances with those obtained from ¹H NMR spectroscopy.⁴ The

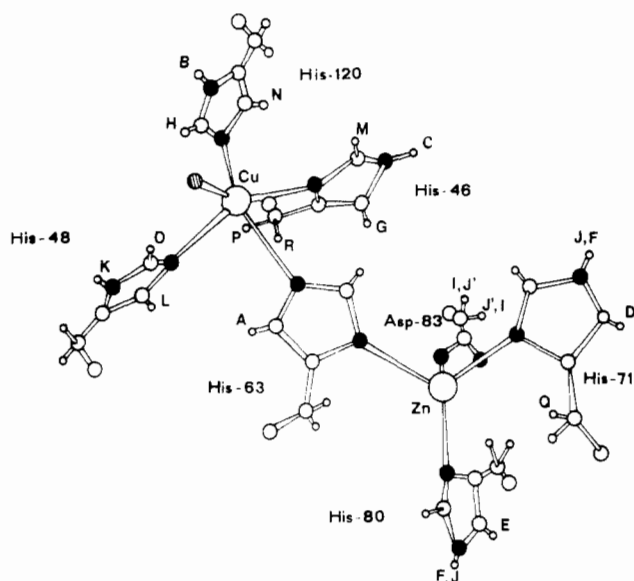
main result was the full assignment of the hyperfine-shifted signals in the ¹H NMR spectra, which, when performed through the analysis of T₁ and T₂ data,⁵ could lead to some misassignment.

- (1) Thanabal, V.; de Ropp, J. S.; La Mar, G. N. *J. Am. Chem. Soc.* **1986**, *108*, 4244.
- (2) Ramaprasad, S.; Johnson, R. D.; La Mar, G. N. *J. Am. Chem. Soc.* **1984**, *106*, 3632.
- (3) Unger, S. W.; LeComte, J. T. J.; La Mar, G. N. *J. Magn. Reson.* **1985**, *64*, 521.
- (4) Banci, L.; Bertini, I.; Luchinat, C.; Piccioli, M.; Scozzafava, A.; Turano, P. *Inorg. Chem.* **1989**, *28*, 4650.

[†] University of Florence.
[‡] University of Bologna.

Table I. Ligand Atom-Copper(II) Distances and Angles for the Coordinated Residues in Bovine SOD^{18,19}

		dist, Å Cu(II)	angle, deg				H ₂ O
			His-46 Nδ1	His-48 Nε2	His-120 Nε2	His-63 Nε2	
His-46	Nδ1	2.04		140	93	77	124
His-48	Nε2	2.14			117	82	93
His-120	Nε2	2.04				157	69
His-63	Nε2	2.06					100
H ₂ O		2.8					

**Figure 1.** Schematic drawing of the copper(II) and zinc(II) binding sites in SOD as deduced from the X-ray structure of the bovine isoenzyme.^{18,19} The numbering of the residues is that of the human isoenzyme.

The T_1 and T_2 data are determined by ligand-centered effects that change from one proton to another.⁵ We are now using the ¹H NOE measurements in order to obtain structural information on the anion derivatives.

The anion binding mode has been a matter of debate owing to the variability of the anion-copper interaction. CN^- , N_3^- , and NCO^- display relatively high affinity and change the electronic and EPR parameters, whereas NCS^- and F^- have little affinity and cause small changes in the spectral parameters.⁶⁻¹⁶

Copper(II) in SOD is bound to four histidines, as shown in Figure 1, according to the X-ray results.^{17,18} Angles and bond distances are reported in Table I.¹⁹ It appears that copper(II)

is exposed to solvent with a water molecule loosely bound.¹⁸ The Cu-O distance may vary from 2.8 Å obtained from an X-ray structure¹⁷⁻¹⁹ to 2.5 Å estimated²⁰ from water ¹H NMR T_1 -¹ measurements²¹ to 2.25 Å obtained from EXAFS measurements.^{22,23} The ¹H NMR spectra of the Cu_2Co_2 derivative have shown that His-48²⁴ has smaller hyperfine shifts for the ring proton signals.²⁵

In order to monitor possible geometric variations of the histidine ligands one with respect to the other upon anion binding, we have performed a ¹H NOE study of the $\text{Cu}_2\text{Co}_2\text{SOD-N}_3^-$ derivative and we have compared the data with those obtained in the absence of azide.⁴ The cyanide derivative is similar in structure to the azide derivative.^{26,27} This is also confirmed by some sample NOE measurements performed during this study (data not shown). On the other hand, NCS^- and F^- have relatively little effects^{13,25} on the ¹H NMR spectrum of $\text{Cu}_2\text{Co}_2\text{SOD}$, and in light of the results obtained on the N_3^- derivative, we believe that NOE's among signals do not change in the case of the latter derivatives. Since the stereochemical disposition of the ligands appears from the ¹H NOE measurements to be similar for the native and azide derivatives, we have tried to improve the quality and the interpretation of the ¹H NOE measurements in order to restrict the uncertainty of the stereochemical variations. The aim is to set the limit for the detection of structural changes. For this reason we have extended the NOE's network including some signals in the diamagnetic region, overlooked up to now, but actually meaningful to relate the histidine positions to the protein frame. Finally, we have discussed the possibilities that make consistent the dramatic spectral changes observed for some anion derivatives⁹⁻¹⁶ with the essentially unaltered histidine positions.

Experimental Section

Bovine erythrocyte $\text{Cu}_2\text{Zn}_2\text{SOD}$ was purchased from Diagnostic Data Inc., Mountain View, CA, and used without further purification. Human SOD was a gift from R. A. Hallewell; it has been obtained from a gene expressed in yeast, according to a previously reported procedure.^{28,29} All reagents were of analytical grade. $\text{Cu}_2\text{Co}_2\text{SOD}$ was obtained according to the reported procedure.^{30,31} All samples have been prepared in 10 mM

- Banci, L.; Bertini, I.; Luchinat, C.; Scozzafava, A. *J. Am. Chem. Soc.* **1987**, *109*, 2328.
- Fee, J. A. In *Oxygen and Oxy-Radicals in Chemistry and Biology*; Rodgers, M. A. J., Power, E. L., Eds.; Academic Press: New York, 1981.
- Valentine, J. S.; Pantoliano, M. W. In *Copper Proteins*; Spiro, T. G., Ed.; Wiley: New York, 1981; Vol. 3, Chapter 8.
- Banci, L.; Bertini, I.; Luchinat, C.; Piccioli, M. *Coord. Chem. Rev.* **1990**, *100*, 67.
- Fee, J. A.; Gaber, B. P. *J. Biol. Chem.* **1972**, *247*, 60.
- Rotilio, G.; Morpurgo, L.; Giovagnoli, C.; Calabrese, L.; Mondovi, B. *Biochemistry* **1972**, *11*, 2187.
- Rotilio, G.; Finazzi-Agrò, A.; Calabrese, L.; Bossa, F.; Guerrieri, P.; Mondovi, B. *Biochemistry* **1971**, *10*, 616.
- Bertini, I.; Borghi, E.; Luchinat, C.; Scozzafava, A. *J. Am. Chem. Soc.* **1981**, *103*, 7779.
- Banci, L.; Bertini, I.; Luchinat, C.; Scozzafava, A.; Turano, P. *Inorg. Chem.* **1989**, *28*, 2377.
- Bertini, I.; Luchinat, C.; Scozzafava, A. *J. Am. Chem. Soc.* **1980**, *102*, 7349.
- Lieberman, R. A.; Sands, R. H.; Fee, J. A. *J. Biol. Chem.* **1982**, *257*, 336.
- Hodgson, E. K.; Fridovich, I. *Biochemistry* **1975**, *14*, 5294.
- Tainer, J. A.; Getzoff, E. D.; Beem, K. M.; Richardson, J. S.; Richardson, D. C. *J. Mol. Biol.* **1982**, *160*, 181.
- Tainer, J. A.; Getzoff, E. D.; Richardson, J. S.; Richardson, D. C. *Nature* **1983**, *306*, 284.
- Richardson, J. S.; Richardson, D. C. Private communication. See also ref 17.

- Bertini, I.; Briganti, F.; Luchinat, C.; Mancini, M.; Spina, G. *J. Magn. Reson.* **1985**, *63*, 41.
- Gaber, B. P.; Brown, R. D., III; Koenig, S. H.; Fee, J. A. *Biochim. Biophys. Acta* **1972**, *271*, 1.
- Blackburn, N. J.; Hasnain, S. S.; Diakun, G. P.; Knowles, P. F.; Binsted, N.; Garner, C. D. *Biochem. J.* **1983**, *213*, 765.
- Blackburn, N. J.; Strange, R. W.; McFadden, L. M.; Hasnain, S. S. *J. Am. Chem. Soc.* **1987**, *109*, 7162.
- Throughout this article we numbered the amino acid residues by following the human isoenzyme sequence, although all the NMR data have been collected on the bovine isoenzyme, for which the X-ray structure is known. Such numbering permits an easier comparison with the many data obtained on the human derivative and its mutants.
- Bertini, I.; Lanini, G.; Luchinat, C.; Messori, L.; Monnanni, R.; Scozzafava, A. *J. Am. Chem. Soc.* **1985**, *107*, 4391.
- Banci, L.; Bertini, I.; Luchinat, C.; Scozzafava, A. *J. Biol. Chem.* **1989**, *264*, 9742.
- Banci, L.; Bertini, I.; Luchinat, C.; Monnanni, R.; Scozzafava, A. *Inorg. Chem.* **1988**, *27*, 107.
- (a) Hallewell, R. A.; Masiarz, F.; Najarian, R.; Puma, J.; Quiroga, M.; Randolph, A.; Sanchez-Pescador, R.; Scandella, C. F.; Smith, B.; Steimer, K.; Müllenbach, G. T. *Nucleic Acids Res.* **1985**, *13*, 2017. (b) Hallewell, R. A.; Mills, R.; Tekamp-Olson, P.; Blacher, R.; Rosenberg, S.; Otting, F.; Masiarz, F. R.; Scandella, C. F. *Biotechnology* **1987**, *5*, 363.
- Banci, L.; Bertini, I.; Luchinat, C.; Hallewell, R. A. *Ann. N.Y. Acad. Sci.* **1988**, *542*, 37.
- Fee, J. A. *J. Biol. Chem.* **1973**, *248*, 4229.

phosphate buffer at pH 7.5, by using either H₂O or D₂O as solvent. Solutions of sodium azide in phosphate buffer at pH 7.5 were prepared in D₂O. Titration of Cu₂Co₂SOD with sodium azide solution was performed in order to obtain a Cu₂Co₂SOD adduct with a saturating amount of azide, according to previously reported data.²⁵

¹H NMR experiments have been performed by using a Bruker MSL 200 instrument. *T*₁ values have been obtained by using either an inversion recovery or a modified DEFT pulse sequence.³²⁻³⁴ All the ¹H NOE experiments have been carried out with the previously reported methodology⁴ or by saturating a signal with a selective pulse. The water signal was suppressed by a superWEFT pulse sequence.³⁵ Reported spectra typically consist of 300 000–1 000 000 scans; they have been collected by block averaging of each 32 768 scans. Exponential multiplication of the free induction decay to improve the signal-to-noise ratio was such to cause a 20-Hz line broadening. The limit of detection for NOE signals ranges from 0.2% to 1%, depending on the signal-to-noise ratio and on the signal line width.

The classical angular overlap model was used for the present system.^{36,37} The calculation program included spin-orbit coupling with $\lambda = 820 \text{ cm}^{-1}$ and a Steven reduction parameter of the orbital contribution equal to 0.78.³⁸ Together with the energy levels, the *g* values and directions were calculated. Finally the *A* values and directions were calculated according to the formalism previously described³⁹ by using $P = 0.027 \text{ cm}^{-1}$ and $K/P = 0.29$,³⁶ where *K* is the Fermi contact constant and *P* is equal to $g_C g_N \mu_B \mu_N \langle r^{-3} \rangle_{av}$.

Results and Discussion

¹H NOE Experiments and Theoretical Considerations. The exchange between free and bound N₃⁻ is fast on the NMR time scale, and therefore the positions of the signals of the N₃⁻ adduct can be related to those of the native enzyme. The titration has been performed in the presence of 10 mM phosphate buffer, i.e. under noninhibitory conditions⁴⁰ and anyway at a concentration much smaller than the reciprocal of the apparent affinity constant of phosphate for the enzyme.⁴¹

NOE is defined as the percent variation of the intensity of a signal when another signal is saturated.^{42,43} The NOE values can be used to obtain interproton distances. Under steady-state conditions (irradiation time of signal *J* > 5*T*₁ of the observed signal *I*) the homonuclear NOE is given by

$$\eta_{IJ} = \frac{\sigma_{IJ}}{\rho_I} \quad (1)$$

where σ_{IJ} is the cross-relaxation between the two protons *I* and *J* and ρ_I is the selective relaxation rate of the observed proton *I*. In the present system ρ_I is equal to the actual *T*₁⁻¹ measured through nonselective techniques, as *T*₁⁻¹ is essentially determined by the hyperfine coupling with the unpaired electrons.^{1-3,44,45} In turn, the cross-relaxation term, σ_{IJ} , is given, in the slow-motion limit that holds in the case of macromolecules, by

$$\sigma_{IJ} = -\frac{\hbar^2 \gamma^4 \tau_c}{10r_{IJ}^6} \quad (2)$$

- (31) Pantoliano, M. W.; Valentine, J. S.; Nafie, L. A. *J. Am. Chem. Soc.* **1982**, *104*, 6310.
 (32) Vold, R. L.; Waugh, J. S.; Klein, M. P.; Phelps, D. E. *J. Chem. Phys.* **1968**, *48*, 3831.
 (33) Levitt, M. H.; Freeman, R. *J. Magn. Reson.* **1979**, *33*, 473.
 (34) Hochmann, J.; Kellerhals, H. P. *J. Magn. Reson.* **1980**, *38*, 23.
 (35) Inubushi, T.; Becker, E. D. *J. Magn. Reson.* **1983**, *51*, 128.
 (36) Schäffer, C. E. *Struct. Bonding (Berlin)* **1968**, *5*, 68.
 (37) Harnung, S. E.; Schäffer, C. E. *Struct. Bonding (Berlin)* **1972**, *12*, 201.
 (38) Banci, L.; Bencini, A.; Bertini, I.; Luchinat, C.; Viezzoli, M. S. *Gazz. Chim. Ital.* **1990**, *120*, 179.
 (39) Bencini, A.; Benelli, C.; Gatteschi, D. *Coord. Chem. Rev.* **1984**, *60*, 131.
 (40) Beyer, W. F.; Wang, Y.; Fridovich, I. *Biochemistry* **1986**, *25*, 6084.
 (41) Mota de Freitas, D.; Luchinat, C.; Banci, L.; Bertini, I.; Valentine, J. S. *Inorg. Chem.* **1987**, *26*, 2788.
 (42) Noggle, J. H.; Schirmer, R. E. *The Nuclear Overhauser Effect*; Academic Press: New York, 1971.
 (43) Neuhaus, D.; Williamson, M. *The Nuclear Overhauser Effect in Structural and Conformational Analysis*; VCH Publ.: New York, 1989.
 (44) Bertini, I.; Luchinat, C. *NMR of Paramagnetic Molecules in Biological Systems*; Benjamin/Cummings: Menlo Park, CA, 1986.
 (45) Banci, L.; Bertini, I.; Luchinat, C.; Piccioli, M. In *NMR and Macromolecular Structure*; Bertini, I., Molinari, H., Nicolai, N., Eds.; VCH Publ.: in press.

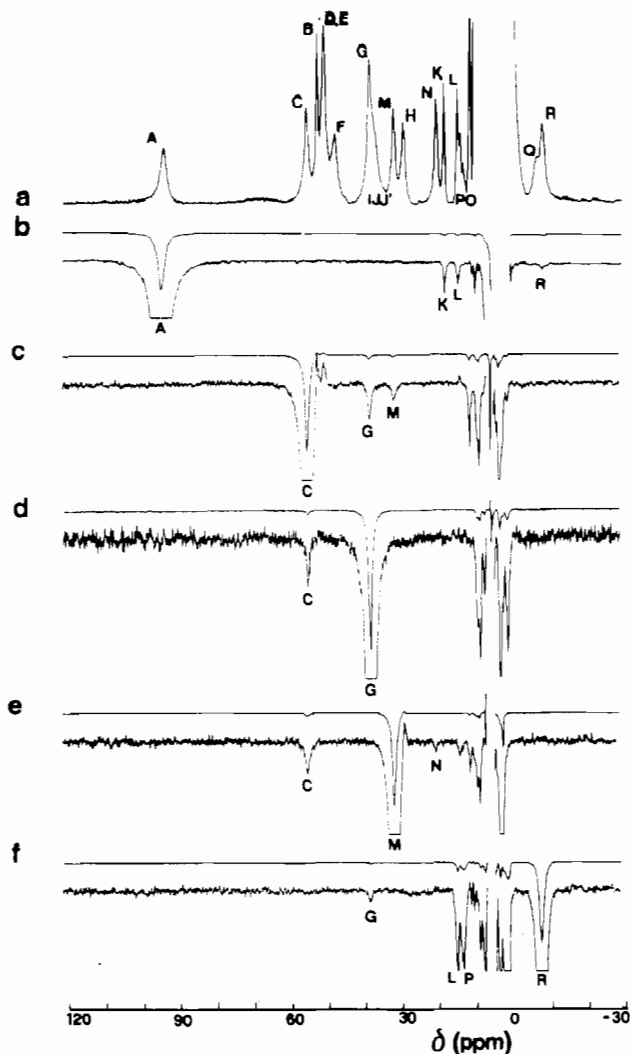


Figure 2. Representative 200-MHz 301 K ¹H NOE difference spectra of the bovine Cu₂Co₂SOD–N₃⁻ adduct: (a) reference spectrum with signals labeled according to the assignment shown in Figure 1; (b–f) difference spectra obtained by saturating signals A (b), C (c), G (d), M (e), and R (f). In the insets the vertical scale is expanded 10 times. All the spectra have been recorded in H₂O. NOE experiments in both H₂O and D₂O have been used for quantitative estimation of NOE values.

where τ_c is the reorientation time of the vector connecting protons *I* and *J* and the other symbols have the usual meaning. As σ_{IJ} is proportional to the square of the dipolar coupling energy, it is proportional to r_{IJ}^{-6} and depends on the correlation time τ_c . This treatment holds for the approximation of an isolated two-spin system. We have checked the validity of the approximation for all the signals of interest by performing a relaxation matrix calculation and found that the differences are negligible with one exception that is discussed later.⁴⁶

The correlation time is provided by the tumbling rate or by any other movement that causes the reorientation of the two spins on a faster time scale. The tumbling time can be estimated, by assuming a globular shape of the protein, through the Stokes–Einstein equation

$$\tau_r = \frac{4\pi\eta r^3}{3kT} \quad (3)$$

where *r* is the average radius of the molecule and η is the solvent viscosity.

We have previously shown⁴ that the anisotropy in τ_r due to the nonspherical shape of the molecule is not so severe. We have, however, faced the problem that the correlation time depends on the protein concentration. This is due to changes in microviscosity

(46) Banci, L.; Bertini, I.; Luchinat, C.; Piccioli, M. *FEBS Lett.*, in press.

Table II. T_1 and NOE Values and Calculated Distances from ^1H NOE Measurements at 200 MHz and 301 K on the Native^a and Azide-Bound Bovine $\text{Cu}_2\text{Co}_2\text{SOD}$ Derivatives

sadt signal	obsd signal	T_1 , ^a ms		$-\eta$, ^b %		calcd dist	
		nat	+N ₃ ⁻	nat	+N ₃ ⁻	nat	+N ₃ ⁻
A (H δ 2(His-63))	L (H δ 2(His-48))	4.3	8.2	0.9 \pm 0.1	1.1 \pm 0.2	2.7 \pm 0.2	2.9 \pm 0.2
A (H δ 2(His-63))	K (H δ 1(His-48))	8.0	17.5	0.6 \pm 0.2	1.1 \pm 0.2	3.2 \pm 0.3	3.3 \pm 0.2
A (H δ 2(His-63))	R (H β 2(His-46))	2.4	4.5	0.2 \pm 0.1	0.3 \pm 0.1	3.3 \pm 0.3	3.2 \pm 0.3
B (H δ 1(His-120))	H (H ϵ 1(His-120))	1.8	2.6	1.0 \pm 0.2	0.9 \pm 0.2	2.3 \pm 0.2	2.5 \pm 0.2
C (H ϵ 2(His-46))	G (H δ 2(His-46))	3.5	3.8	1.4 \pm 0.2	2.1 \pm 0.2	2.4 \pm 0.2	2.3 \pm 0.2
C (H ϵ 2(His-46))	M (H ϵ 1(His-46))	2.7	2.9	0.9 \pm 0.1	0.8 \pm 0.2	2.5 \pm 0.2	2.5 \pm 0.2
G (H δ 2(His-46))	C (H ϵ 2(His-46))	4.2	4.4	1.7 \pm 0.4	1.4 \pm 0.2	2.4 \pm 0.2	2.5 \pm 0.2
M (H ϵ 1(His-46))	C (H ϵ 2(His-46))	4.2	4.4	2.2 \pm 0.4	1.5 \pm 0.1	2.4 \pm 0.2	2.3 \pm 0.2
M (H ϵ 1(His-46))	N (H δ 2(His-120))	2.9	3.7		0.5 \pm 0.1		2.9 \pm 0.3
R (H β 2(His-46))	G (H δ 2(His-46))	3.5	3.8	0.6 \pm 0.2	0.6 \pm 0.2	2.8 \pm 0.3	2.8 \pm 0.3
Q (H β 1(His-71))	D (H δ 2(His-71))	3.8	5.1	1.4 \pm 0.2	1.2 \pm 0.1	2.4 \pm 0.2	2.6 \pm 0.2
L (H δ 2(His-48))	α^c (γ 1CH ₃ (Val-118))	70	120	33 \pm 6	48 \pm 9	2.8 \pm 0.3	2.9 \pm 0.3
N (H δ 2(His-120))	x^d (H β 2(His-120))			9 \pm 1	4 \pm 0.5		
R (H β 2(His-46))	P (H β 1(His-46))	1.6	5.5	5.4 \pm 0.8	5.9 \pm 1.0	1.7 \pm 0.2	2.0 \pm 0.2
P (H β 1(His-46))	R (H β 2(His-46))	2.4	4.5	9.0 \pm 1.0		1.7 \pm 0.2	
L (H δ 2(His-48))	P (H β 1(His-46))	1.6	5.5	1.3 \pm 0.3		2.2 \pm 0.2	
P (H β 1(His-46))	L (H δ 2(His-48))	4.3	8.2	5.5 \pm 1		2.0 \pm 0.2	
L (H δ 2(His-48))	R (H β 2(His-46))	2.4	4.5	0.5 \pm 0.1	1.3 \pm 0.3	2.6 \pm 0.3	2.6 \pm 0.2
R (H β 2(His-46))	L (H δ 2(His-48))	4.3	8.2	2.3 \pm 0.2	4.0 \pm 0.8	2.3 \pm 0.2	2.3 \pm 0.2

^a T_1 for the signal on which NOE is detected. ^b All NOE values have been normalized at infinite diluted solution; i.e., $\tau_r = 1.4 \times 10^{-8}$ s. ^c Signal α is in the diamagnetic region at 0.5 ppm in the native derivative and at 0.9 ppm in the N₃⁻ adduct. ^d Signal x is at 11.1 ppm in the native derivative and at 13.1 ppm in the N₃⁻ adduct.

in highly concentrated protein solutions.⁴⁷ An equation of the type

$$\tau_r = \frac{\tau_{r0}}{1 - (r/(D - r))^3} \quad (4)$$

where r is the average protein radius, τ_{r0} is the tumbling time of the protein calculated at infinite dilution, and D is the distance between two protein centers, is available in the relaxometry literature⁴⁷ to account for the variation of τ_r with concentration. Owing to the uncertainty in the concentration, we have made an independent estimate of the correlation time by measuring the NOE between signals C and G, and C and M (Figure 2), belonging to the rigid frame (known distances) of a histidine ring. This has allowed us to normalize to the same effective correlation time independent samples of different microviscosity of both inhibited and noninhibited enzyme. For the less concentrated samples the τ_r values (1.6×10^{-8} s) were in good agreement with the 1.4×10^{-8} s obtained from the Stokes-Einstein equation. The highest value obtained with the above procedure was 2.15×10^{-8} s for 8 mM protein concentration, consistent with eq 4.

The NOE's observed for the azide derivative are reported in Table II and compared with those of the native enzyme. Some representative difference spectra are reported in Figure 2. The errors on distances are estimated from the errors on NOE's, T_1 's, and τ_r . Such errors range between ± 0.1 and ± 0.3 Å. These values tell us that the relative positions of the histidines have not changed substantially, and the errors provide the degree of indetermination within the present state of advancement of the investigation tools.

We have tried also some transient NOE's. Owing to the fast relaxation rates of the isotropically shifted signals, it has been possible to invert signals only partially, unless the selectivity of the pulse is lost. Under these conditions the transient NOE is less efficient than steady-state experiments.⁴⁶ On the other hand, transient NOE experiments give the same results as steady-state experiments, contrary to what was recently reported.⁴⁸

Discussion of the ^1H NOE Results. Among the NOE's reported in Table II, we were particularly interested in the NOE's between signals of protons of different histidines in such a way to monitor conformational variations upon azide binding. From inspection

of Table II it appears that whereas the NOE's vary from unligated to N₃⁻ derivative, the distances between proton pairs are essentially equal or similar. The NOE between M (H ϵ 1 of His-46) and N (H δ 2 of His-120) can be observed only in the N₃⁻ derivative because these signals become sufficiently separated only when N₃⁻ binds. Therefore, the corresponding value for the native protein is not available. However, the distance obtained from NOE measurements on the N₃⁻ adduct is consistent with the X-ray structure of the native enzyme. Also, signals Q and R are not resolved in the native enzyme whereas they are resolved in the N₃⁻ derivative. It is possible, therefore, to show that Q gives a NOE to D whereas R gives NOE's to P, L, and G and responds to irradiation of A, thus leading to unambiguously assign R as H β 2 of His-46⁴ and Q as one of the β -protons of one histidine coordinated to Co(II). The X-ray data are of help in this respect and permit a tentative assignment of signal D. The calculated interproton distance of 2.6 Å between protons Q and D is consistent with their assignment to H β 1 and H δ 2 protons of His-71, respectively.

The NOE's between A and L and A and K in the azide adduct provide the information that the distance between protons of His-63 and of His-48 could only change within 0.2 Å. Owing to the small difference in chemical shift values of signals L and P in the azide adduct, it has not been possible to quantitatively monitor the NOE between these two signals. Nevertheless, it has been possible, through a procedure previously reported⁴⁹ designed to minimize the off-resonance effects, to qualitatively detect a sizeable NOE between L and P. This experiment is indicative that also the distance between H δ 2 of His-48 and H β 1 of His-46 is not essentially changed upon azide binding.

The comparison with the NOE's of the azide and native derivatives (see Table II) provides a feeling of the degree of freedom of His-48 with respect to the diamagnetic frame upon azide binding. Signal L gives a NOE, both in the native and the azide adduct, with a signal in the diamagnetic region located at 0.5 ppm in the native enzyme. Owing to its intensity, it can be reasonably assigned to a methyl group. The signal moves from 0.5 to 0.9 ppm in the fully formed azide adduct. A NOE has been measured at different irradiation times of signal L on the native derivative, on the azide adduct, and on a sample with 50% of both species. These measurements show that no sizeable variation occurs also in this proton-proton distance. A possible candidate for this signal

(47) Koenig, S. H. In *Water in Polymers*; Rowland, S. P., Ed.; ACS Symposium Series 127; American Chemical Society: Washington, DC, 1980; p 157.

(48) Paci, M.; Desideri, A.; Sete, M.; Falconi, M.; Rotilio, G. *FEBS Lett.* **1990**, *2*, 231.

(49) Banci, L.; Bertini, I.; Luchinat, C.; Viezzoli, M. S. *Inorg. Chem.* **1990**, *29*, 1438.

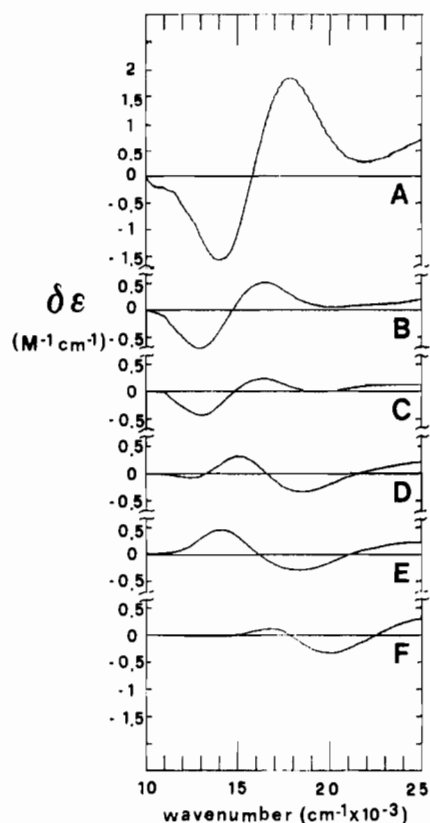


Figure 3. Visible and near-infrared CD spectra of human $\text{Cu}_2\text{Zn}_2\text{SOD}$ (B) and its anion derivatives of thiocyanate (C), cyanate (D), azide (E), and cyanide (F). The CD spectrum of the Ile-137 mutant (A) is also shown.

is $\gamma\text{-I-CH}_3$ of Val-118, which, in the X-ray structure, is at 2.12 Å from $\text{H}\delta 2$ of His-48. Also, signal N gives rise to a strong NOE with a peak at 13.1 ppm in the azide derivative; this effect has been also detected on a signal at 11.1 ppm in the absence of azide. The signal at 13.1 ppm in the azide derivative also experiences a NOE from signal M. A reasonable candidate for this signal is $\text{H}\beta 2$ of His-120.

From the above discussion it appears that the histidines bound to copper can move only little, if at all, upon azide binding. Within this frame there are two features to be noted. (i) The distance between $\text{H}\beta 1$ of His-46 (signal P) and $\text{H}\beta 2$ of His-46 (signal R) is calculated, in the azide adduct, longer than required for geminal CH_2 protons, if the same τ_c as that for the other proton pairs is used. We believe that a shorter τ_c is effective as a result of CH_2 mobility. (ii) The distance between $\text{H}\delta 2$ of His-48 (signal L) and $\text{H}\beta 2$ of His-46 (signal R) is shorter, outside the experimental error, when measured upon irradiation of signal R rather than upon irradiation of signal L. This behavior can be explained by taking into account that $\text{H}\beta 2$ of His-46 (signal R) is more strongly coupled to $\text{H}\beta 1$ of His-46 (signal P) than to $\text{H}\delta 2$ of His-48 (signal L). In this three-spin system, coupling of $\text{H}\beta 2$ of His-46 with $\text{H}\beta 1$ of His-46 is a further cross-relaxation pathway that increases the NOE on L, as can be derived from reported equations.^{43,46}

Discussion of the Structure of the Anion Derivatives. The observation of NOE's on the ^1H NMR spectra of the azide derivative of $\text{Cu}_2\text{Co}_2\text{SOD}$ shows that the overall relative spatial disposition of the histidines involved in the coordination to copper does not change significantly. This holds also for the cyanide adduct owing to the similarity of the spectra^{26,27} and similar sample NOE's and presumably for the NCO^- derivative, since the shifts are intermediate between those of the azide and those obtained in the absence of anions. The fluoride and thiocyanate derivatives show ^1H NMR spectra similar to that of the uninhibited derivative.

On the other hand, the electronic and EPR spectra of the CN^- , N_3^- , and NCO^- derivatives are considerably different from each other. Table III shows the EPR parameters¹² and electronic transition energies, measured from CD spectra (Figure 3), of the

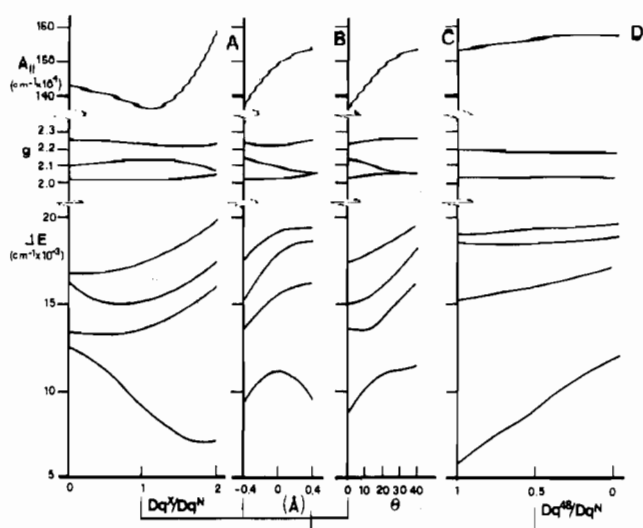


Figure 4. Transition energies, g values, and $A_{||}$ values of the native SOD calculated with $Dq(\text{N})$ of His-120, His-63, and His-46 = 2170 cm^{-1} , $Dq(\text{N})$ of His-48 = 1085 cm^{-1} , and $e_{\sigma}/e_{\pi} = 0.13$. The geometric coordinates are those in Table I. The variations of the above values are calculated as a function of (A) the Dq value of a fifth ligand (X) with the same polar angles as those of the native water molecule, (B) the movement of the copper ion toward and beyond the average plane formed by N(His-120), N(His-63), and N(His-46) in the presence of X ($Dq(\text{X})$ taken as 2170 cm^{-1}), (C) the θ angle formed by the Cu-X direction with the perpendicular to the average plane formed by N(His-120), N(His-63), and N(His-46), and (D) the Dq value of N(His-48), in the presence of the X ligand at the water position. The conditions are the same as at the right side of (B). The arrows represent values calculated with the same parameters.

anion adducts of $\text{Cu}_2\text{Zn}_2\text{SOD}$. The CD spectra obtained in this work refer to the human isoenzyme. They are essentially the same as those previously reported on some derivatives of the bovine isoenzyme.^{25,31} For the cyanide derivative of the human isoenzyme a further band at $17.0 \times 10^3\text{ cm}^{-1}$ is detected. The single-crystal EPR data on the native bovine isoenzyme are also shown.¹⁵ In order to make some meaningful considerations, we include in the discussion the mutant Ile-137 of the human isoenzyme.⁵⁰ The large Ile residue makes the cavity hydrophobic, and no water is present in the cavity nearby the copper ion.

The high-energy feature in the CD spectra of the copper(II) ion decreases in energy from CN^- to N_3^- , to NCO^- , and to the native derivative, whereas the spectra of the NCS^- and F^- derivatives are similar to those of the native enzyme. The Ile-137 mutant, without coordinated water, shows somewhat higher energies than the native enzyme. This has been interpreted,^{38,50} as due to a stronger His-48 to copper coordination bond.

The ^1H NMR spectra of the $\text{Cu}_2\text{Co}_2\text{SOD}$ anion derivatives indicate that the protons of His-48 experience hyperfine coupling with the unpaired electrons to different extents (Table IV). The chemical shifts decrease smoothly from the Ile-137 to the CN^- derivative. For example, if the hyperfine coupling value of signal L ($\text{H}\delta 2$ of His-48) is taken as zero in the cyanide derivative, it increases to 3.4 ppm in the N_3^- derivative and to 6.5 and 14.7 ppm in the presence of NCO^- and NCS^- , respectively. In the native enzyme, where a water molecule is weakly coordinated, the above parameter is 19.3 ppm, and it results to be 28.9 ppm in the absence of water (Ile-137 derivative).

In order to rationalize the observed trend in the EPR and CD properties of the inhibitor derivatives of $\text{Cu}_2\text{Zn}_2\text{SOD}$ within the constraints of the NOE results, we attempted some ligand field calculations with the angular overlap model scheme using a Dq value of 2170 cm^{-1} for N(His-120), N(His-46), and N(His-63), half of that value for N(His-48), and $e_{\pi}/e_{\sigma} = 0.13$. The Dq of the water ligand was set to zero. For the histidine residues we

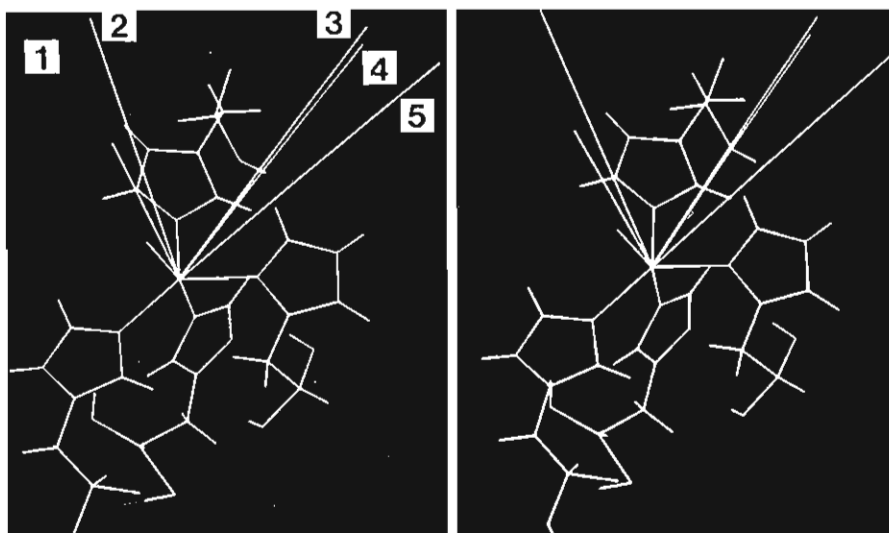


Figure 5. Stereoview of the copper(II) site of native SOD.^{18,19} The imidazolate rings belong to His-120 (rear), His-46 (right), His-63 (front), and His-48 (left). The water molecule is on the upper left side. Vectors 1 and 4 represent the experimental $g_{||}$ directions obtained from single-crystal EPR spectra of the native enzyme^{15,18} (1) and of the cyanide derivative (4). Vectors 2, 3, and 5 show the $g_{||}$ directions calculated from an angular overlap model analysis³⁶ of the native enzyme (2) and its new positions obtained either by increasing Dq of the X ligand to twice Dq of the regularly coordinated histidines as in Figure 4A (5) or by moving the copper ion toward the mean square plane of the N_3X chromophore as in Figure 4B (3).

Table III. EPR Parameters^a and Visible Electronic Transitions^b of Cu_2Zn_2SOD , Its Inhibitor Derivatives, and the Ile-137 Mutant

	g_z	g_x^c	g_y^c	$A_{ }, 10^4 \text{ cm}^{-1}$	trans energies, ^b 10^{-3} cm^{-1}	
HSOD Ile-137	2.25	2.04		162	14.3	17.5
Nat SOD ^d	2.26	2.03	2.09	142	13.0	16.4
SOD + F ⁻	2.26	2.06		143	13.0	16.5
SOD + NCS ⁻	2.25	2.06		148	13.0	16.3
SOD + NCO ⁻	2.26	2.05		158	12.8	15.3, 18.2
SOD + N ₃ ⁻	2.24	2.04		157	14.1	18.3
SOD + CN ⁻	2.21	2.05		188	17.0	19.9

^a The EPR parameters are obtained from powderlike room-temperature solution spectra at X-band, unless otherwise indicated. The data are relative to the bovine isoenzyme unless otherwise indicated. ^b The electronic transitions have been obtained from a best fitting of the CD spectra with Gaussian functions. The data are relative to the human isoenzyme. ^c The X-band spectra are treated as axial. The single g values reported for the perpendicular feature approximately correspond to the average between g_x and g_y . ^d The EPR parameters are those of the single-crystal analysis.¹⁵ The corresponding values for the human isoenzyme $g_{||} = 2.26$, $g_{av} = 2.05$, and $A_{||} = 142 \times 10^4 \text{ cm}^{-1}$. The transition energies are for the human isoenzyme.

Table IV. 200-MHz Room-Temperature ¹H NMR Shifts of His-48 Imidazole Protons of Derivatives of Cu_2Co_2SOD

Cu_2Co_2SOD derivatives	$\delta(H\delta 1)$ signal K, ppm	$\delta(H\delta 2)$ signal L, ppm	$\delta(H\epsilon 1)$ signal O, ppm
HSOD Ile-137	38.6	38.0	22.5
HSOD	34.6	28.3	19.6
BSOD	34.5	28.4	19.6
BSOD + F ⁻	31.3	25.6	18.2
BSOD + NCS ⁻	27.7	23.8	16.4
BSOD + NCO ⁻	19.8	15.6	14.3
BSOD + N ₃ ⁻	15.9	12.5	10.5
BSOD + CN ⁻	13.0	9.1	<11

^a These data are relative to a 4 M solution of F⁻ in the presence of 2 mM Cu_2Co_2SOD . The adduct is not fully formed.

used an anisotropic π interaction perpendicular to the imidazole planes. The above parameters were shown to satisfactorily reproduce the electronic transition energies and EPR parameters of the native enzyme.³⁸ In a first series of calculations (Figure 4A) the Dq of a ligand X in the position of the weakly coordinated water has been increased from zero to twice the Dq of the regularly coordinated histidines. In two other series of calculations performed by setting the Dq of X equal to that of the other three histidines, the position of copper has been moved toward and

beyond the plane formed by N(His-120), N(His-46), and N(His-63) (Figure 4B) or the X ligand has been lowered toward the N(His-120), N(His-46), and N(His-63) plane (Figure 4C). In every case the average of the three highest transitions increases, $A_{||}$ increases except at the beginning of the perturbation of Figure 4A ($Dq(X)/Dq(N(\text{His-120})) < 1$), and g_{\perp} becomes more axial, while $g_{||}$ shows smaller variations. We should notice that the direction of $g_{||}$ in the native system has been already reproduced.³⁸ The direction of $g_{||}$ in the CN⁻ adduct is also known.¹⁵ In Figure 5 the computed and observed $g_{||}$ directions are shown for the final values of cases shown in Figure 4A,B. It appears that both perturbations move the $g_{||}$ direction close to the experimental one of the cyanide adduct, the departures being 15 and 8° for cases A and B, respectively. The perturbation of Figure 4C also moves $g_{||}$ in the right direction but to a much smaller extent.

These calculations show that a strong fifth ligand in the original position of water plus either a movement of copper or a lowering of this ligand toward the plane of the other three histidines can account for the general trend. Further information comes from the analysis of the hyperfine shifts experienced by His-48. The hyperfine shifts depend on unpaired electron spin density on the coordinated nitrogen, which, in turn, depends on the angle of the Cu-N(His-48) direction with the $g_{||}$ (or $A_{||}$) direction. Figure 5 shows that His-48 passes from a value of about 100° for such an angle to about 160° in the cyanide derivative. This can account for a large decrease of the hyperfine coupling; however, in low-symmetry systems like the present one, some sizeable hyperfine coupling is still expected. We feel that a decrease in hyperfine coupling as large as that observed in the case of CN⁻ is due to a simultaneous lengthening of the Cu-N(His-48) distance. In every square-pyramidal system containing copper(II) the apical ligand is more weakly coordinated than the equatorial ones.⁵¹ The movement conceived in Figure 4B is more consistent with the ¹H NOE data if the Cu-N(His-48) distance increases. At this point it is meaningful to discuss the T_1 values of His-48 protons in the azide derivative (Table II) (the corresponding values of the cyanide adduct are not available, since the signals are deep inside the diamagnetic region). The T_1 values of histidine protons in the absence of sizeable contact hyperfine couplings are mainly due to dipolar proton-metal-centered unpaired electron coupling.⁴⁴ Metal-proton distances can be calculated if the correlation time is known. Such time, which corresponds to the electronic relaxation time, has been estimated from the T_1 values of the other

(51) Hathaway, B. J. In *Comprehensive Coordination Chemistry*; Pergamon: Oxford, England, 1987; Vol. 5, Chapter 53, 533.

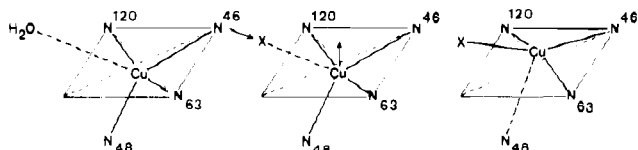


Figure 6. Scheme of the reciprocal movement of the copper ion and the X ligand: chromophore in the native enzyme (left); final arrangement in the case of a strong ligand (right).

protons to be 2×10^{-11} s.⁵ The T_1 values of His-48 protons in the N_3^- derivative are consistent with a Cu-N distance of 2.7 Å, i.e. with a lengthening of about 0.6 Å. This value is sizeably higher than the value of 0.27 Å estimated from EXAFS studies,²³ but the metal to nitrogen distance is less than 20% different. A factor of 2 in the electronic relaxation time could make the two figures coincident. Note that T_1 of signal L passes from 4.3 ms in the case of the native derivative to 8.2 ms in the azide derivative. Furthermore, signal P, corresponding to Hβ1 of His-46, experiences a Cu-H distance increase of about the same amount (T_1 is 1.6 ms in the native derivative and 5.5 ms in the azide derivative). Despite that indeterminism in the Cu-H distances may be relatively high, the increase in Cu-N(His-48) distance is a conceivable geometrical perturbation that may occur together with other geometrical variations. Figure 4D shows the effect of a variation of Dq of the His-48 ligand under the conditions of the right-hand side of Figure 4B, i.e., with copper being approximately in the average X, N(His-120), N(His-48), and N(His-63) plane. The effects of detaching His-48 are relatively small but in the right direction (increase of $A_{||}$ and transition energies).

From heteronuclear NMR studies it has been suggested that $F^{-12,13,52}$ and $NCS^{-12,14}$ are actually bound to copper. Spectro-

scopic data on both Cu_2Zn_2SOD and Cu_2Co_2SOD and ligand field calculations are consistent with a small bonding interaction around the water binding position. The hyperfine shifts of His-48 are most sensitive to such binding; when no ligand is present at the water position as in the case of the Ile-137 mutant, His-48 is better bound. Azide and cyanide seem to bind quite tightly and to cause detachment of His-48 through a movement of copper. This can be schematically envisaged as in Figure 6. Cyanate has an intermediate behavior; its CD spectrum, which reveals a further transition, can be consistent with an even more distorted geometry.

Concluding Remarks. The 1H NOE study of Cu_2Co_2SOD in the presence of saturating amounts of azide has shown that the interproton distances of the histidines bound to copper, and between such histidines and diamagnetic groups, are essentially the same upon azide binding. The technique of NOE in paramagnetic molecules has been pushed to its limits in order to minimize the errors. Within this frame the spectroscopic properties of the anion derivatives have been discussed on the basis of an angular overlap approach that takes into consideration the movement of copper and the binding strength and position of the anions. The $A_{||}$ trend, $g_{||}$ values and directions, electronic transitions in the Cu_2Zn_2 derivatives, and T_1 values of the protons of His-48 and His-46 in Cu_2Co_2SOD point to a lengthening of the Cu-N(His-48) distance from NCS^- to CN^- ligands. This trend is consistent with the EXAFS report on the SOD anion derivatives.²³

Registry No. L-His, 71-00-1; N_3^- , 14343-69-2; CN^- , 57-12-5; NCO^- , 661-20-1; NCS^- , 302-04-5; F^- , 16984-48-8; Cu, 7440-50-8; superoxide dismutase, 9054-89-1.

(52) Viglino, P.; Rigo, A.; Stevanato, R.; Ranieri, G. A.; Rotilio, G.; Calabrese, L. *J. Magn. Reson.* **1979**, *34*, 265.

Contribution from the Fujian Institute of Research on the Structure of Matter and Fuzhou Laboratory of Structural Chemistry, Chinese Academy of Sciences, Fuzhou, Fujian 350002, China

Syntheses, Structures, and Properties of Vanadium, Cobalt, and Nickel Compounds with 2-Mercaptophenol

Beisheng Kang,* Linghong Weng, Hanqin Liu, Daxu Wu, Liangren Huang, Cenzhong Lu, Jinghua Cai, Xuetai Chen, and Jiayi Lu

Received April 20, 1989

Three new compounds of 2-mercaptophenolate (mp^{2-}), trinuclear $(Et_4N)[V_3(mp)_6]$ (**1a**) or $(Ph_4P)[V_3(mp)_6]$ (**1b**), dimeric $(Et_4N)_2[Co(mp)(Hmp)]_2$ (**2**), and binuclear $(Et_4N)_2[Ni_2(mp)_2(Hmp)]_2$ (**3**), were synthesized and their structures determined. Compound **1b** crystallizes in the triclinic space group $P\bar{1}$ with $a = 14.127$ (4) Å, $b = 14.342$ (4) Å, $c = 15.878$ (4) Å, $\alpha = 65.08$ (2)°, $\beta = 73.09$ (2)°, $\gamma = 78.68$ (2)°, $V = 2781.3$ Å³, and $Z = 2$. Compound **2** crystallizes in the monoclinic space group $P2_1/c$ with $a = 16.606$ (2) Å, $b = 15.575$ (1) Å, $c = 17.725$ (2) Å, $\beta = 111.07$ (1)°, $V = 4277.8$ Å³, and $Z = 4$. Compound **3** crystallizes in the monoclinic space group $P2_1/n$ with $a = 9.179$ (4) Å, $b = 17.487$ (5) Å, $c = 12.840$ (4) Å, $\beta = 92.87$ (3)°, $V = 2058.6$ Å³, and $Z = 2$. Structural analyses revealed the multifunctional chelating character of mp^{2-} : it can be S_2O_4 (t for terminal) as in **2**, **3**, and $(Et_4N)_2[Fe_2(mp)_4]^{13}$ (**4**), S_2O_6 (b for bridging) as in **1b** and **4**, or S_2OH as in **3**. Some structural regularities are observed. Compounds **1b** and **2** are paramagnetic with magnetic moments of 2.76 and 2.38 μ_B per molecule in the polycrystalline state, respectively. Compound **2** dissociates in DMSO to its monomer, which is rapidly oxidized by trace air. The final product is purple $[Co(mp)_2]^-$ with a magnetic moment of 3.26 μ_B . A simulated 1H NMR spectrum of **3** revealed the nuclear spin coupling of the hydrogen atom in the hydroxyl group with the ortho H on the same phenyl ring.

Introduction

Transition-metal elements are essential to many biological systems in nature. For example, the recently identified second nitrogenase¹ contains vanadium in an O_3S_3 environment.² The development of V chemistry has also been furthered by the desire to understand its biological role in organisms such as tunicates,³ which contain tunicchrome⁴ (TC) with V(III) chelated to polypeptide chains rich in hydroxyl groups. While four- or five-coordinate Co(II) thiolates have been considered as models for the catalytic site of the cobalt-substituted alcohol dehydrogenase,⁵

the V, Co, Cr, Mn, and Cu complexes of EHPG [ethylenebis-[(*o*-hydroxyphenyl)glycine]] have been studied as models for metallotransferrins.^{6,7} Nickel is known to be present in the

* To whom correspondence should be addressed at the Fujian Institute of Research on the Structure of Matter.

- (1) (a) Robson, R. L.; Eady, R. R.; Richardson, T. H.; Miller, R. W.; Hawkins, M.; Postgate, J. R. *Nature (London)* **1986**, *322*, 388. (b) Arber, J. M.; Dodson, B. R.; Eady, R. R.; Stevens, P.; Hasnain, S. S.; Garner, C. D.; Smith, B. E. *Ibid.* **1987**, *325*, 372. (c) Smith, B. E.; Eady, R. R.; Lowe, D. J.; Gormal, C. *Biochem. J.* **1988**, *250*, 299.
- (2) George, G. N.; Coyle, C. L.; Hales, B. J.; Cramer, S. P. *J. Am. Chem. Soc.* **1988**, *110*, 4057.
- (3) Kustin, K.; McLeod, G. C.; Gilbert, T. R.; Briggs, L. R. *Struct. Bonding (Berlin)* **1983**, *53*, 139.
- (4) Oltz, E. M.; Bruening, R. C.; Smith, M. J.; Kustin, K.; Nakanishi, K. *J. Am. Chem. Soc.* **1988**, *110*, 6162.
- (5) Corwin, D. J., Jr.; Fikar, R.; Koch, S. A. *Inorg. Chem.* **1987**, *26*, 3079.